Research Article

Hashim M. Alshehri*

Influence of decaying heat source and temperature-dependent thermal conductivity on photo-hydro-elasto semiconductor media

https://doi.org/10.1515/phys-2025-0145
received November 26, 2024; accepted March 13, 2025

Abstract: This research examines the impact of varying thermal conductivity within the framework of generalized photo-thermoelastic theory in a thermo-hydrodynamic semiconductor material. The changes in thermal conductivity are presented to evaluate the wave distributions of temperature, carrier density, excess pore water pressure, stress, and displacement in a poroelastic (poro-silicon, PSi) material. The integrated model of thermoelasticity, hydro-mechanics, and plasma waves is examined. The normal mode analysis is employed to provide the analytical solution of the distribution of the researched fields as components of this phenomenon. The findings are demonstrated about the effects of the thermal conductivity parameter as the heat source decays. A comparison of the numerical results with prior analytical studies is conducted, excluding the new parameter, and the behaviors of physical quantities in the numerical solutions are analyzed to validate the accuracy of the proposed technique. All physical quantities are influenced by changing thermal conductivity.

Keywords: decaying heat source, photo-thermoelasticity, thermal conductivity, porosity, silicon, hydrodynamic

Nomenclature

C_e	specific heat of the medium
C_s	heat capacity of semiconductor grains
C_w	heat capacity of pore water
D_E	carrier diffusion coefficient
E_g	energy gaps
e_{ij}	strain tensor
e	cubical dilatation
g	gravity
K_0	thermal conductivity
k_d	coefficient of permeability
N	carrier concentration (density)
n_o	porosity
m	volumetric heat capacity of medium
P	excess pore water pressure
T_0	reference temperature
t	time variable
T	absolute temperature
u_i	displacement vector
λ,μ	Lame's parameters
$\delta_n = (3\lambda + 2\mu)d_n$	deformation potential coefficient
$\gamma = (3\lambda + 2\mu)\alpha_s$	thermal expansion of volume
α_s	thermal expansion coefficient of semiconductor grains
ρ_s	density of semiconductor grains
ρ_w	density of pore water
ρ	density of the medium
τ	lifetime
τ_0	thermal memory
α_w	thermal expansion coefficient of pore water
σ_{ij}	stress tensor

1 Introduction

The importance of semiconductor materials arises from their recent applications, particularly in contemporary technology and emerging energy alternatives. The thermoelastic hypothesis, prevalent in engineered structural materials, is crucial for steel stress analysis and applied mechanical sciences. The increase in body temperature results not only from internal and external heating sources but also from deformations occurring during the micro-inertia of the microelement. Numerous applications rely on analyzing

* Corresponding author: Hashim M. Alshehri, Mathematics Department, Faculty of Science, King Abdulaziz University, Jeddah, 21521, Saudi Arabia, e-mail: hmalshehri@kau.edu.sa

the effects of sunlight or laser beams on the external surfaces of semiconductor materials [1,2], disregarding the internal structures of the media. Semiconductor materials have solely been examined as elastic materials, disregarding the impact of light beams on them. Semiconducting materials are classified as nanoparticles in contemporary technology, with several applications, such as industrial photovoltaic solar cells. Electronic and elastic deformations arise when a laser beam impinges onto the surface of a semiconductor material. Due to advancements in semiconductor integrated circuit technologies solid-state sensor technologies have been extensively utilized across various domains, characterized by their compact size, lightweight nature, and low energy consumption. To comprehend the internal structural characteristics of elastic media, particularly in semiconductor materials, it is essential to examine their electrical properties while taking into account their mechanical and thermal attributes [3,4]. The significance of semiconducting materials arises from their recent applications in numerous advantageous technologies, particularly those centered on new energy alternatives. Numerous applications rely on examining the impact of sunlight or laser beams on the exterior surface of semiconducting materials, disregarding the interior structure of the medium. In this instance, certain surface electrons will be stimulated, resulting in the generation of photo-excited free carriers. The connection between photothermal (PT) theory and semiconductors is significant in contemporary technology. Numerous scientists have employed the PT hypothesis to ascertain temperature values. The thermal diffusion of nanocomposite semiconductor materials has been quantified.

An improved representation of thermoelastic disturbances is provided by generalized thermoelasticity, a state-of-the-art model that takes into account the mechanical and thermal interactions between materials. In contrast to the classical model, the velocities at which these disturbances propagate as waves are more in line with those of the actual world [5]. This shortcoming has led to the development of many non-classical thermoelastic theories, such as the Lord-Shulman (LS) model [6]. To better explain thermoelastic behavior in complicated contexts, these models include more variables [7–9]. The temperature-dependent thermal conductivity in convective-radiative fins is one of the many aspects of this link that researchers have looked into extensively [10]. In addition to these, they have looked into methods of identification [11], solved the thermoelasticity problem in an axisymmetric construction [12], and studied the interplay of thermoelasticity in a hollow cylinder [13]. Lotfy [14] investigated the two-dimensional Mode-I crack thermoelastic problem using fiber-reinforced materials. There has been a lot of research on wave propagation using generalized thermoelasticity as a framework [15–19].

Electrons are excited when exposed to a laser or sunlight, which causes plasma waves to form. This causes the plasma wave, the elastic wave, and the thermal wave to interact with one another. In building the PT theory, Gordon *et al.* [20] and Kreuzer [21] accomplished astounding things. Research on the PT theory of thermoelastic-electronic wave coupling was conducted by Mandelis *et al.* [22]. In a semiconducting medium, Todorovic [23] studied plasmaelastic and thermoelastic waves. A reflection problem in a semiconducting medium was investigated by Song *et al.* [24] to determine the ratios of reflection coefficients. Within the framework of LS theory, Hosseini and Zhang [25] clarified the wave propagation issue in a semiconducting medium. At the interface of a thermoelastic micropolar cubic crystal and a semiconducting half-space, Ailawalia *et al.* [26] examined the effect of mechanical force. A two-dimensional semiconducting medium according to the LS model was investigated by Hobiny and Abbas [27] using thermoelastic theory. Waves in a semiconducting medium were investigated by Liu *et al.* [28] in the absence of body force using a thermophysical properties characterization. A new model for investigating PT interaction in a spinning microstretch semiconductor medium subjected to initial stress was proposed by Lotfy *et al.* [29]. Recent research has significantly advanced the understanding of the interactions between thermal, optical, and magnetic effects in semiconductor materials. Raddadi *et al.* [30] investigated the optoelectronic–thermomagnetic effect in a microelongated non-local rotating semiconductor subjected to pulsed laser heating with varying thermal conductivity, offering valuable insights into the behavior of such materials under dynamic conditions. Building on this, Elamin *et al.* [31] explored the response of a photo-elasto-electric semiconductor porous medium with changing thermal conductivity and two-temperature effects, shedding light on the complex thermal and mechanical interactions within these materials.

Experiencing high temperatures causes an elastic material's thermal conductivity to change experimentally. Hence, maintaining a constant heat conductivity is not an option. To investigate stacked thin plates with varied thermal conductivity, Youssef and El-Bary [32] presented a mathematical model. Researchers Ezzat and Youssef [33] tested the notion of one relaxation time on thermoelastic media with varying electrical and thermal conductivities. The effects of changing thermal conductivity in an elastic half-space on fractional thermoelasticity theory were investigated by Sherief and Abd El-Latief [34]. The thermal stress of a hollow cylinder in a thermoelastic media that depends on temperature was determined by Zenkour and Abbas [35] using the finite element method. In the framework of the dual-phase-lag and L-S thermoelasticity models, Yasein *et al.* [36]

showed how changing the thermal conductivity of a semiconducting material subjected to a thermal ramp type affects the material. In their study, Abbas *et al.* [37] examined the effects of varying thermal conductivity on a semiconducting medium including cylindrical cavities. For a porous medium with varying heat conductivity, the heat transfer behavior becomes spatially dependent, requiring the thermal conductivity to be treated as a function of position within the medium to accurately model temperature distribution and heat flow. To investigate PT interactions in a semiconductor with mechanical ramp type and variable thermal conductivity, Lotfy and El-Bary [38] put forward an elastic-thermodiffusion model.

More research is needed to understand the thermo-hydro-mechanical (THM) coupled behavior of unsaturated soil, which is prevalent [39]. Wave propagation in thermoelastic porous media is a topic of study for engineers working in petroleum, chemicals, pavements, and nuclear waste management. A lot of studies have been conducted on it. Research by Kumar and Devi [40] examined several heat sources in a generalized thermoelastic media that was both porous and subjected to thermomechanical boundary conditions. To represent generalized thermoelasticity in poroelastic materials, Sherief and Hussein [41] created governing equations in their research. Subsequently, a half-space thermal shock issue was resolved using this model. A two-dimensional porous material problem with a single relaxation time was solved by Abbas and Youssef [42] using fractional order generalized thermoelasticity theory. At the planar interface between two different materials, one being a homogeneous, isotropic thermoelastic material, and the other a porous medium, the interaction of thermal and mechanical properties must be carefully considered. Wei *et al.* [43] investigated the refraction and reflection of a longitudinal wave with an oblique incidence. In a thorough investigation, Schanz [44] examined the analytical solutions and poro-elastodynamic models. Additionally, the author contrasted numerical approaches using finite elements and boundary elements [45]. Previous fluid-saturated medium research inspired our analysis. Theories have evolved from Biot's simple isotropic poroelastic theory to a whole framework for dealing with phenomena and material anisotropy [46]. The Booker and Savvidou [47] analytical solution for soil consolidation considers a point source and an impermeable, rigid, spherical heat source. Biot proposed a thermodynamics theory for elastic saturated porous materials [48]. Xiong *et al.* [49] used normal mode analysis to study the poroelastic generalized thermoelasticity. Recent studies have made significant contributions to the understanding of the dynamic behavior of porous and fiber-reinforced materials under various thermal, magnetic, and mechanical effects. Gupta *et al.* [50] developed a double poro-magneto-thermoelastic model incorporating microtemperatures and initial stress, which provided insight into memory-dependent heat transfer in such systems. Similarly, Dutta *et al.* [51] investigated the behavior of nonlocal fiber-reinforced double porous materials under fractional-order heat and mass transfer, expanding the understanding of heat and mass transport in complex materials. Further, Dutta *et al.* [52] explored the impact of nonlocal effects on shear wave propagation in fiber-reinforced poroelastic structures under impulsive disturbances. Meghana *et al.* [53] presented a size-dependent analysis of surface wave propagation in fractured porous seabeds subjected to fractional-order derivatives, providing new insights into wave behavior in such media. Das *et al.* [54] examined the effects of fractional-order derivatives on wave reflection in pre-stressed microstructured solids with dual porosity, advancing the understanding of wave dynamics in porous materials. Additionally, Gupta *et al.* [55] studied the response of moisture and temperature diffusivity in orthotropic hygro-thermo-piezo-elastic media, highlighting the effects of moisture and temperature on the material properties.

The primary objective of this study is to investigate the impact of temperature-dependent thermal conductivity and a decaying heat source on wave propagation phenomena in hydro-elasto-semiconductor media within the framework of generalized photo-thermoelasticity theory. Specifically, the study aims to analyze the effects of these factors on the distribution of temperature, carrier density, stress, displacement, and excess pore water pressure. Additionally, the study seeks to validate the proposed model by comparing the results with prior analytical studies that did not account for variable thermal conductivity and decaying heat sources. The main hypotheses of this study are that the inclusion of temperature-dependent thermal conductivity significantly alters the interactions between thermal, mechanical, and plasma waves, leading to distinct temperature and stress distributions compared to models assuming constant conductivity. Additionally, it is hypothesized that the decaying heat source causes a substantial attenuation of thermal waves, thereby affecting the coupled fields of temperature, carrier density, and mechanical stresses. Furthermore, the combined effect of variable thermal conductivity and a decaying heat source is expected to enhance the accuracy of wave propagation predictions in hydro-semiconductor media, making them more consistent with observed physical behaviors. These hypotheses aim to deepen the understanding of coupled THM–plasma interactions in semiconductor materials.

The goal of the current study is to determine how the variability of thermal conductivity values affects a hydro-semiconducting material. The linked THM plasma model is examined utilizing normal mode analysis during decaying

heat sources. A poroelastic half-space covering the semiconducting half-space has been used to model the problem. The analytical elements of displacement, stress, excess pore water pressure, plasma carrier density, and distribution of temperature are derived from the application of specific boundary conditions to the poro-semiconductor medium. All examined physical quantities were found to be contingent upon changing thermal conductivity. This research enhances the theoretical framework of thermoelasticity, applicable to the design and optimization of structures and materials under elevated temperatures. After that, the data were utilized to contrast and compare the two methods: the photo-thermoelastic dynamic (PTD) model and the combined photo-thermo-hydro-mechanical dynamic (PTHMD) model.

2 Mathematical model and basic equations

Consider a half-space with plasm diffusion (carrier density N) in a poroelastic semiconductor. In addition, the coordinate system (x, y, z) is considered, where the z-axis is taken in the downward direction from the vertical. The fundamental governing formulas are provided for a hydro-semiconducting (homogeneous, isotropic, and porous) medium in the following form:

(i) The photo-excited process of semiconductor poroelastic medium establishes a connection between thermal and plasma waves [48,49]

$$D_{\mathrm{E}}\nabla^2 N - \frac{\partial N}{\partial t} - \frac{N}{\tau} + \kappa\, T = 0, \tag{1}$$

where the quantity κ denotes the thermal activation coupling parameter.

(ii) The photo-thermoelastic theory applies equations of motion to elastic semiconductor materials, taking into account thermo-plasma-hydromechanical coupling [38,41]

$$(\lambda + \mu)\nabla(\nabla\cdot\vec{u}) + \mu\nabla^2\vec{u} - \nabla P - \gamma\nabla T - \delta_n\nabla N = \rho\ddot{\vec{u}}. \tag{2}$$

(iii) For poroelastic semiconductors, the heat conduction equation is based on thermal conductivity variations [33,38]

$$\nabla.\,(K\nabla T) - m\left(1 + \tau_0\frac{\partial}{\partial t}\right)\frac{\partial T}{\partial t} - \gamma T_o\left(1 + \tau_o\frac{\partial}{\partial t}\right)\frac{\partial e}{\partial t} + \frac{E_{\mathrm{g}}}{\tau}N = 0. \tag{3}$$

(iv) The equation for water's mass conservation is [47–49]

$$b_{\mathrm{w}}\left(\alpha_{\mathrm{w}}\frac{\partial T}{\partial t} - \frac{\partial e}{\partial t}\right) - \rho_{\mathrm{w}}\frac{\partial^2 e}{\partial t^2} + \nabla^2 P = 0, \tag{4}$$

where $m = n_0\rho_{\mathrm{w}}C_{\mathrm{w}} + (1 - n_o)\rho_{\mathrm{s}}C_{\mathrm{s}}$ and $b_{\mathrm{w}} = \frac{g\rho_{\mathrm{w}}}{k_d}$.

The constitutive governing equation is [32,36]

$$\sigma_{iI} = \lambda u_{r,r}\,\delta_{iI} + \mu u_{I,i} + \mu u_{i,I} - (P + \gamma T - \delta_n N)\delta_{iI}. \tag{5}$$

Given that thermal conductivity exhibits a linear relationship in temperature as demonstrated in [32]

$$K(T) = K_0(1 + K_1 T). \tag{6}$$

According to Eq. (6), K_1 can be chosen as a small negative parameter (variable thermal conductivity parameter) and K_0 expresses the thermal conductivity in a natural case (temperature independent [ambient thermal conductivity]). This linear approximation is widely used in semiconductor physics because it effectively captures the influence of phonon scattering and carrier-phonon interactions, which cause thermal conductivity to either increase or decrease with temperature depending on the material's characteristics. For semiconductors, higher temperatures generally enhance phonon scattering, reducing thermal conductivity. The chosen form provides a balance between accuracy and analytical tractability, allowing us to investigate the coupled effects of thermal conductivity variations and decaying heat sources on wave propagation phenomena in hydro-semiconductor media. On the other hand, the Kirchhoff transformation formula can be expressed in an integral form of thermal conductivity [32] as follows:

$$\tilde{T} = \frac{1}{K_0}\int_0^T K(\chi)\mathrm{d}\chi. \tag{7}$$

Combining the differentiation technique with the transformation map, Eq. (7) according to the space coordinates x_i yields [38]

$$K_0\tilde{T}_{,i} = K(T)T_{,i} \Rightarrow K_0\tilde{T}_{,ii} = (K(T)T_{,i})_{,i},\ K_0\dot{\tilde{T}} = K\dot{T}. \tag{8}$$

When the nonlinear terms are ignored, Eq. (8) can be rewritten as

$$\begin{aligned} K_0\tilde{T}_{,ii} &= K_{,i}T_{,i} + KT_{,ii} = K_0(1 + K_1T)_{,i}T_{,i} + KT_{,ii} \\ &= K_0K_1(T_{,i})^2 + KT_{,ii} = KT_{,ii}. \end{aligned} \tag{9}$$

Operating by the differential operator $\frac{\partial}{\partial x_i}$ on both sides of plasma-heat, Eq. (1) using Eq. (8) yields

$$\frac{\partial}{\partial x_i}\left(D_E\nabla^2 - \frac{\partial}{\partial t} - \frac{1}{\tau}\right)N + \frac{\kappa K_0}{K}\frac{\partial\tilde{T}}{\partial x_i} = 0. \tag{10}$$

Taylor expands is applied for the last term of Eq. (10) with linearity property, which yields

$$\begin{aligned}\frac{\kappa K_0}{K_0(1+K_1T)}\frac{\partial\tilde{T}}{\partial x_i} &= \kappa(1+K_1T)^{-1}\frac{\partial\tilde{T}}{\partial x_i} = \kappa(1-K_1T \\ &\quad + (K_1T)^2 - \ldots\ldots)\frac{\partial\tilde{T}}{\partial x_i} \\ &= \kappa\frac{\partial\tilde{T}}{\partial x_i} - \kappa K_1T\frac{\partial\tilde{T}}{\partial x_i} + \kappa(K_1T)^2\frac{\partial\tilde{T}}{\partial x_i} \\ &\quad - \ldots\ldots = \kappa\frac{\partial\tilde{T}}{\partial x_i}.\end{aligned} \tag{11}$$

Eq. (10), according to the linearity form of Eq. (11), can be rewritten as

$$\left(D_E\nabla^2 - \frac{\partial}{\partial t} - \frac{1}{\tau}\right)N + \kappa\,\tilde{T} = 0. \tag{12}$$

By applying the map transformations defined in Eqs. (7) and (8), Eq. (3) can be reformulated as:

$$\nabla^2\tilde{T} - \left(1+\tau_o\frac{\partial}{\partial t}\right)\left(\frac{m}{K_0}\frac{\partial\tilde{T}}{\partial t} + \frac{\gamma T_o}{K_0}\frac{\partial e}{\partial t}\right) + \frac{E_g}{K_0\tau}N = 0. \tag{13}$$

The waves are thought to be moving on the xz- plane. Therefore, in a poro-semiconducting material, the vector of displacement $\vec{u}$ is formulated in two dimensions (2D) as $\vec{u} = (u, 0, w)$; $u = u(x, z, t)$, $w = w(x, z, t)$, $e = \frac{\partial u}{\partial x} + \frac{\partial w}{\partial z}$.

The 2D analysis of motion Eq. (2) according to the variable thermal conductivity (map transform) takes the following form:

$$\begin{aligned}&(\lambda+\mu)\frac{\partial e}{\partial x} + \mu\left(\frac{\partial^2u}{\partial x^2} + \frac{\partial^2u}{\partial z^2}\right) - \frac{\partial P}{\partial x} - \gamma\frac{\partial\tilde{T}}{\partial x} - \delta_n\frac{\partial N}{\partial x} \\ &\quad = \rho\frac{\partial^2u}{\partial t^2},\end{aligned} \tag{14}$$

$$\begin{aligned}&(\lambda+\mu)\frac{\partial e}{\partial z} + \mu\left(\frac{\partial^2w}{\partial x^2} + \frac{\partial^2w}{\partial z^2}\right) - \frac{\partial P}{\partial z} - \gamma\frac{\partial\tilde{T}}{\partial z} - \delta_n\frac{\partial N}{\partial z} \\ &\quad = \rho\frac{\partial^2w}{\partial t^2}.\end{aligned} \tag{15}$$

On the other hand, the constitutive Eq. (5) takes the following form:

$$\sigma_{xx} = 2\mu\frac{\partial u}{\partial x} + \lambda e - \gamma\tilde{T} - P + (3\lambda+2\mu)d_nN, \tag{16}$$

$$\sigma_{zz} = 2\mu\frac{\partial w}{\partial x} + \lambda e - \gamma\tilde{T} - P + (3\lambda+2\mu)d_nN, \tag{17}$$

$$\sigma_{xz} = \mu\left(\frac{\partial w}{\partial x} + \frac{\partial u}{\partial z}\right), \tag{18}$$

where $\delta_n = (3\lambda+2\mu)d_n$, d_n represents the electronic deformation coefficient. In this problem, two photo-thermoelasticity theories are described, the first is the classical coupled theory when $\tau_o = 0$ and the second is the LS model that appears when $\tau_o > 0$.

We also utilize the dimensionless quantities in the context of the mapped temperature shown below for purposes of simplicity:

$$\left.\begin{aligned}&\bar{N} = \frac{\delta_n}{2\mu+\lambda}N, \quad \bar{x}_i = C_0\xi x_i, \quad \bar{u}_i = C_0\xi u_i, \quad \bar{t} = C_0^2\xi t, \\ &(\bar{\tau}, \bar{\tau}_o) = C_0^2\xi(\tau, \tau_o), \quad \bar{\tilde{T}} = \frac{\gamma}{2\mu+\lambda}\tilde{T}, \quad \bar{\sigma}_{ij} = \frac{\sigma_{ij}}{\mu}, \\ &\bar{P} = \frac{P}{2\mu+\lambda}, \quad \xi = \frac{m}{K_0}, \quad C_0^2 = \frac{\lambda+2\mu}{\rho}.\end{aligned}\right\} \tag{19}$$

Applying the dimensionless Eq. (19), the main Eqs. (4) and (12)–(18) are converted into the following formulations under the map transformations when omitting the primes for simplicity:

$$\left(\nabla^2 - \varepsilon_1 - \varepsilon_2\frac{\partial}{\partial t}\right)N + \varepsilon_3\tilde{T} = 0, \tag{20}$$

$$\nabla^2u + (B^2-1)\frac{\partial e}{\partial x} - B^2\left(\frac{\partial P}{\partial x} + \frac{\partial\tilde{T}}{\partial x} + \frac{\partial N}{\partial x}\right) = B^2\frac{\partial^2u}{\partial t^2}, \tag{21}$$

$$\nabla^2w + (B^2-1)\frac{\partial e}{\partial z} - B^2\left(\frac{\partial P}{\partial z} + \frac{\partial\tilde{T}}{\partial z} + \frac{\partial N}{\partial z}\right) = B^2\frac{\partial^2w}{\partial t^2}, \tag{22}$$

$$\nabla^2\tilde{T} + \varepsilon_7N + \left(\frac{\partial}{\partial t} + \tau_o\frac{\partial^2}{\partial t^2}\right)(\tilde{T} + \varepsilon_8e) = 0, \tag{23}$$

$$\nabla^2P = \varepsilon_4\frac{\partial e}{\partial t} + \varepsilon_5\frac{\partial\tilde{T}}{\partial t} + \varepsilon_6\frac{\partial^2e}{\partial t^2}, \tag{24}$$

$$\sigma_{xx} = 2\frac{\partial u}{\partial x} + \frac{\lambda}{\mu}e - B^2(\tilde{T} + P - N), \tag{25}$$

$$\sigma_{zz} = 2\frac{\partial w}{\partial z} + \frac{\lambda}{\mu}e - B^2(\tilde{T} + P - N), \tag{26}$$

$$\sigma_{xz} = \frac{\partial w}{\partial x} + \frac{\partial u}{\partial z}. \tag{27}$$

In the above equations, the main coefficients are

$$\begin{aligned}&\varepsilon_1 = \frac{1}{\tau\,D_E\xi C_0^2}, \quad \varepsilon_2 = \frac{1}{D_E\xi C_0^2}, \quad \varepsilon_3 = \frac{\kappa\delta_n}{D_EC_0^4\gamma\xi^2}, \\ &\varepsilon_4 = \frac{b_w}{\lambda+2\mu}, \quad \varepsilon_5 = -\frac{b_w\alpha_w}{\rho\xi}, \quad \varepsilon_6 = -\frac{\rho_w}{\rho}, \\ &B^2 = \frac{\lambda+2\mu}{\mu}, \quad \varepsilon_7 = \frac{\gamma E_g}{\tau m\delta_n}, \\ &\varepsilon_8 = \frac{\gamma^2T_0}{m(\lambda+2\mu)}, \quad \nabla^2 = \frac{\partial^2}{\partial x^2} + \frac{\partial^2}{\partial z^2}.\end{aligned}$$

When we apply the differentiation properties to the solutions of Eqs. (15) and (16), we obtain

$$\left(\nabla^2 - \frac{\partial^2}{\partial t^2}\right)e - \nabla^2(P + \tilde{T} + N) = 0. \tag{28}$$

3 Solution to the problem

In semiconductor and materials science, normal mode analysis is often applied to study wave propagation, thermal distributions, and elastic responses, particularly when the medium is subjected to various physical fields like thermal, magnetic, or mechanical influences. By analyzing the normal modes, researchers can derive important information about the system's natural frequencies, damping characteristics, and response to external excitations, which is crucial for designing and optimizing materials for specific engineering applications. To get a solution for the physical variables previously mentioned, we apply the following normal mode analysis [33,38]:

$$[N, e, P, \tilde{T}, \sigma_{ij}](x, y, t) = [N^*, e^*, P^*, \tilde{T}^*, \sigma_{ij}^*](x)\exp(\omega t + ibz), \tag{29}$$

where ω is the complex time constant, b represents the wave number in the z-direction, and the quantities $(N^*, e^*, P^*, T^*, \sigma_{ij}^*)(x)$ are the amplitude of the main physical fields. The following equations are obtained in coupled form by using the solutions provided by Eq. (29) in Eqs. (20), (23), (24), (28), (25), and (26) according to mapped temperature as follows:

$$(D^2 - \alpha_1)N^* + \varepsilon_3\,\tilde{T}^* = 0, \tag{30}$$

$$(D^2 - \alpha_2)e^* - (D^2 - b^2)(\tilde{T}^* + P^* + N^*) = 0, \tag{31}$$

$$(D^2 - \alpha_3)\tilde{T}^* + \varepsilon_7 N^* + \alpha_4 e^* = 0, \tag{32}$$

$$(D^2 - b^2)P^* - \alpha_5 e^* - \alpha_6\tilde{T}^* = 0, \tag{33}$$

$$\sigma_{xx}^* = 2Du^* + \frac{\lambda}{\mu}e^* - B^2(\tilde{T}^* + P^* - N^*), \tag{34}$$

$$\sigma_{zz}^* = 2ibw^* + \frac{\lambda}{\mu}e^* - B^2(\tilde{T}^* + P^* - N^*), \tag{35}$$

where $\frac{\mathrm{d}}{\mathrm{d}x} = D$, $\alpha_1 = b^2 + \varepsilon_1 + \omega\,\varepsilon_2$, $\alpha_2 = b^2 + \omega^2$, $\alpha_3 = b^2 + \omega + \tau_0\omega^2$, $\alpha_4 = \alpha_3\varepsilon_8$, $\alpha_5 = \omega(\varepsilon_4 + \omega\varepsilon_6)$, $\alpha_6 = \omega\varepsilon_5$.

The following sixth-order differential equation is obtained by solving these coupled Eqs. (30)–(33)

$$(D^6 - E_1D^4 + E_2D^2 - E_3)\{N^*, \tilde{T}^*, e^*, P^*\}(x) = 0. \tag{36}$$

where

$$E_1 = \alpha_1 + \alpha_2 + \alpha_3 + \alpha_5 - \alpha_4, \tag{37}$$

$$E_2 = A_1 + A_2 + \alpha_2(\alpha_1 + \alpha_3) - \alpha_4(\alpha_1 + b^2) + \alpha_4\varepsilon_3, \tag{38}$$

$$E_3 = \alpha_2A_1 + A_3 + \alpha_4b^2(\varepsilon_3 - \alpha_1), \tag{39}$$

$$A_1 = \alpha_1\alpha_3 - \varepsilon_3\varepsilon_7, \quad A_2 = \alpha_5(\alpha_1 + \alpha_3) + \alpha_4\alpha_6. \tag{40}$$

Eq. (36) can be put in the following factorization form:

$$(D^2 - k_1^2)(D^2 - k_2^2)(D^2 - k_3^2)\{N^*, \tilde{T}^*, e^*, P^*\}(x) = 0. \tag{41}$$

The roots $k_n^2 (n = 1,\ 2,\ 3)$ of Eq. (41) can be chosen in real-positive values. Using radiation conditions $(N^*, e^*, P^*, \tilde{T}^*, \sigma_{ij}^*)(x) \to 0$ when $x \to \infty$, the solution of Eq. (36) can be rewritten in linear form as follows:

$$\{\tilde{T}^*, N^*, e^*, P^*\}(x) = \sum_{n=1}^{3} M_n\{1, a^*, b^*, c^*\}e^{-k_nx}, \tag{42}$$

where $a_n^* = \frac{-\varepsilon_3}{k_n^2 - \alpha_1}$, $b_n^* = -\frac{k_n^4 - (\alpha_1 + \alpha_3)k_n^2 + A_1}{\alpha_4(k_n^2 - \alpha_1)}$, $c_n^* = \frac{-\alpha_5k_n^4 + A_2k_n^2 - A_3}{\alpha_4(k_n^2 - \alpha_1)(k_n^2 - b^2)}$, and the expressions M_n $(n = 1,\ 2,\ 3)$ are defined as unknown parameters that can be obtained from boundary conditions.

After using the normal mode approach, the horizontal and vertical displacement components can be decreased in the following manner, using Eqs. (21) and (22).

$$u^*(x) = \Gamma(b, \omega)e^{-lx} + \sum_{n=1}^{3}\frac{M_nk_n}{(k_n^2 - l^2)}\left\{\begin{aligned}&B^2\left(\frac{\alpha_5k_n^4 - A_2k_n^2 + A_3}{\alpha_4(k_n^2 - \alpha_1)(k_n^2 - b^2)} + \frac{\varepsilon_3}{k_n^2 - \alpha_1} - 1\right)\\ &+ (1 - B^2)\left(\frac{k_n^4 - (\alpha_1 + \alpha_3)k_n^2 + A_1}{\alpha_4(k_n^2 - \alpha_1)}\right)\end{aligned}\right\}e^{-k_nx}, \tag{43}$$

$$\begin{aligned}e = \frac{\partial u}{\partial x} + \frac{\partial w}{\partial z} \Rightarrow e^* = Du^* + ibw^* \Rightarrow w^* = \frac{i}{b}(Du^* - e^*)\\ = \frac{-i}{b}\left[l\Gamma e^{-lx} + \sum_{n=1}^{3}\frac{M_nk_n^2}{(k_n^2 - l^2)}\left\{\begin{aligned}&B^2\left(\frac{\alpha_5k_n^4 - A_2k_n^2 + A_3}{\alpha_4(k_n^2 - \alpha_1)(k_n^2 - b^2)} + \frac{\varepsilon_3}{k_n^2 - \alpha_1} - 1\right)\\ &+ (1 - B^2)\left(\frac{k_n^4 - (\alpha_1 + \alpha_3)k_n^2 + A_1}{\alpha_4(k_n^2 - \alpha_1)}\right) - \frac{b_n^*(k_n^2 - l^2)}{k_n^2}\end{aligned}\right\}e^{-k_nx}\right].\end{aligned} \tag{44}$$

The expressions of mechanical stresses components can be rewritten as

$$\sigma_{xx}^{*}(x) = -2l\Gamma e^{-lx} + \sum_{n=1}^{3} \frac{2M_n k_n^2}{(k_n^2 - l^2)} \left\{ \begin{array}{l} B^2 \left(1 - \dfrac{\alpha_5 k_n^4 - A_2 k_n^2 + A_3}{\alpha_4 (k_n^2 - \alpha_1)(k_n^2 - b^2)} - \dfrac{\varepsilon_3}{k_n^2 - \alpha_1} \right) \\ + \left(\dfrac{k_n^4 - (\alpha_1 + \alpha_3) k_n^2 + A_1}{\alpha_4 (k_n^2 - \alpha_1)} \right) \left((B^2 - 1) - \dfrac{\lambda (k_n^2 - l^2)}{2 k_n^2 \mu} \right) \\ - \dfrac{B^2 (k_n^2 - l^2)}{2 k_n^2} \left(1 - \dfrac{\alpha_5 k_n^4 - A_2 k_n^2 + A_3}{\alpha_4 (k_n^2 - \alpha_1)(k_n^2 - b^2)} + \dfrac{\varepsilon_3}{k_n^2 - \alpha_1} \right) \end{array} \right\} e^{-k_n x}, \tag{45}$$

$$\sigma_{zz}^{*}(x) = l^2 \Gamma e^{-lx} + \sum_{n=1}^{3} \frac{M_n b^2}{(k_n^2 - l^2)} \left\{ \begin{array}{l} B^2 \left(\dfrac{\alpha_5 k_n^4 - A_2 k_n^2 + A_3}{\alpha_4 (k_n^2 - \alpha_1)(k_n^2 - b^2)} + \dfrac{\varepsilon_3}{k_n^2 - \alpha_1} - 1 \right) \\ + \left(\dfrac{k_n^4 - (\alpha_1 + \alpha_3) k_n^2 + A_1}{\alpha_4 (k_n^2 - \alpha_1)} \right) \left(B^2 - \dfrac{\lambda (k_n^2 - l^2)}{2 b^2 \mu} - 1 \right) \\ - \dfrac{B^2 (k_n^2 - l^2)}{b_n^2} \left(1 - \dfrac{\alpha_5 k_n^4 - A_2 k_n^2 + A_3}{\alpha_4 (k_n^2 - \alpha_1)(k_n^2 - b^2)} + \dfrac{\varepsilon_3}{k_n^2 - \alpha_1} \right) \end{array} \right\} e^{-k_n x}, \tag{46}$$

where $l^2 = b^2 + B^2\omega^2$ and $\Gamma(b, \omega)$ expresses an unknown parameter.

4 Boundary conditions

The following boundary THM plasma conditions (which are applied on the poro-semiconductor surface at $x = 0$) are used to evaluate the constants $M_n(n = 1, 2, 3)$ and $\Gamma(b, \omega)$ [56,57]:

(1) The half-space surface is subjected to a thermal shock that varies with time. The fact that the intensity of a thermal shock for mapped temperature wave changes and weakens over time must be taken into account:

$$\tilde{T}(0, z, t) = T_0 e^{-\upsilon t} \exp(\omega t + ibz). \tag{47}$$

By removing the decaying parameter υ, the resulting waveform would be a constant-amplitude thermal shock waveform. This exponential decay function was chosen to represent a heat source that diminishes progressively over time, capturing the natural attenuation of heat in many physical systems. The sensitivity of the results to this decay function is significant, as the decay rate υ directly influences the attenuation speed of thermal waves and, consequently, the distributions of temperature, carrier density, and mechanical stresses.

(2) The following condition may be used for the excess pore water pressure, which can be chosen freely on the free surface:

$$P(0, z, t) = 0. \tag{48}$$

(3) Due to the thermal shock that varies with time and the diffusion process inside the poro-semiconductor, the carrier density can reach the hydro-semiconductor boundary before recombination. In this case, the carrier density according to the equilibrium carrier concentration N_0 can be expressed as follows:

$$N(0, z, t) = N_0. \tag{49}$$

(4) On the outer surface of the hydro-semiconductor medium, the mechanical boundary condition can be taken during the loaded force with constant value Ω_1 as

$$\sigma_{xx}(0, z, t) = \Omega_1(z, t) = -\Omega_1^{*} \exp(\omega t + ibz). \tag{50}$$

By employing the conventional mode approach to Eqs. (41)–(44), the subsequent set of equations was identified

$$\sum_{n=1}^{3} M_n(b, \omega) = T_0 e^{-\upsilon t}, \tag{51}$$

$$\sum_{n=1}^{3} \left(\frac{-\alpha_5 k_n^4 + A_2 k_n^2 - A_3}{\alpha_4 (k_n^2 - \alpha_1)(k_n^2 - b^2)} \right) M_n = 0, \tag{52}$$

$$-\sum_{n=1}^{3} \frac{\varepsilon_3}{k_n^2 - \alpha_1} M_n = N_0^{*}, \tag{53}$$

$$-2l\,\Gamma+\sum_{n=1}^{3}M_n\frac{2k_n^2}{(k_n^2-l^2)}\begin{Bmatrix}B^2\left(1-\dfrac{\alpha_5k_n^4-A_2k_n^2+A_3}{\alpha_4(k_n^2-\alpha_1)(k_n^2-b^2)}-\dfrac{\varepsilon_3}{k_n^2-\alpha_1}\right)\\+\left(\dfrac{k_n^4-(\alpha_1+\alpha_3)k_n^2+A_1}{\alpha_4(k_n^2-\alpha_1)}\right)\left((B^2-1)-\dfrac{\lambda(k_n^2-l^2)}{2k_n^2\mu}\right)\\-\dfrac{B^2(k_n^2-l^2)}{2k_n^2}\left(1-\dfrac{\alpha_5k_n^4-A_2k_n^2+A_3}{\alpha_4(k_n^2-\alpha_1)(k_n^2-b^2)}+\dfrac{\varepsilon_3}{k_n^2-\alpha_1}\right)\end{Bmatrix}=-\Omega_1^*. \tag{54}$$

After solving the above system of Eqs. (51)–(54) using the matrix inverse procedure, the unknown constants $M_n(n = 1,\ 2,\ 3)$ and Γ can be obtained [58]. From Eqs. (6) and (7), the gradient temperature according to normal mode analysis can be rewritten in the following form:

$$T^* = \frac{1}{K_1}[\sqrt{1+2K_1\tilde{T}^*}-1]. \tag{55}$$

5 Numerical results and discussion

PSi can be treated as a hydro-porous semiconducting medium, with the corresponding constant values listed in Table 1. The MATLAB program is used with numerical simulations to achieve the analytical and numerical solutions that were obtained. Table 1 shows the physical constants for PSi material, which are measured in SI units according to previous studies [38–44].

Figure 1 shows the effect of the decaying heat parameter on the wave propagation distributions of temperature, carrier density, horizontal and vertical displacements, mechanical stress, and excess pore water pressure in a poroelastic semiconductor medium. All computational results were analyzed within the framework of photo-thermoelasticity theory, incorporating variable thermal conductivity. The numerical results reveal significant insights into the coupled behavior of these physical quantities under the influence of thermal decay. According to the temperature distribution, the decaying heat parameter was found to directly affect the temperature distribution within the medium and satisfy the boundary condition. As the decaying heat parameter increases, the temperature gradient becomes steeper near the heat source, resulting in a faster diffusion of thermal energy. This leads to a more rapid attenuation of the temperature wave as it propagates through the medium [59]. Furthermore, the incorporation of variable thermal conductivity enhances the complexity of the temperature field, making the heat dissipation rate highly sensitive to spatial variations in conductivity, which appears in Figure 2. On the other hand, the carrier density, which governs the semiconductor's electrical properties, is influenced by the thermal field due to the thermo-electric coupling. The numerical results show that an increase in the decaying heat parameter leads (Figure 1) to a more localized carrier density distribution. As the heat dissipates more rapidly with a higher decaying parameter, the thermal excitation of carriers reduces in the outer regions, causing a decrease in the spread of carriers from the heat source. This is

Table 1: Physical constants of PSi medium

Unit	Symbol	Value	Unit	Symbol	Value
N/m^2	λ	3.64×10^{10}	N	p	100
	μ	5.46×10^{10}			
kg/m^3	ρ_s	2.3×10^3	$1/cm^3$	N_0	9.65×10^9
K	T_0	800	kg/m^3	ρ_w	10^3
s	τ	5×10^{-5}	m/s	k_d	10^{-8}
m^3	d_n	-9×10^{-31}	J/kg K	C_w	4×10^3
m^2/s	D_E	2.5×10^{-3}	$°C^{-1}$	α_w	2×10^{-4}
eV	E_g	1.11	J/kg K	C_s	6×10^2
K^{-1}	α_s	4.14×10^{-6}	J/kg K	C_e	695
$Wm^{-1}K^{-1}$	K	150	s	τ_o	0.0002
kg/m^3	ρ	2,000	$\Omega_1^* = 0.5$	$\theta_1 = 300$ K	$n_0 = 0.4$
$\omega = \omega_0 + i\xi$	$\omega_0 = -2$	$\xi = 0.001$	$i = \sqrt{-1}$	$t = 0.02$ s	$b = 1$

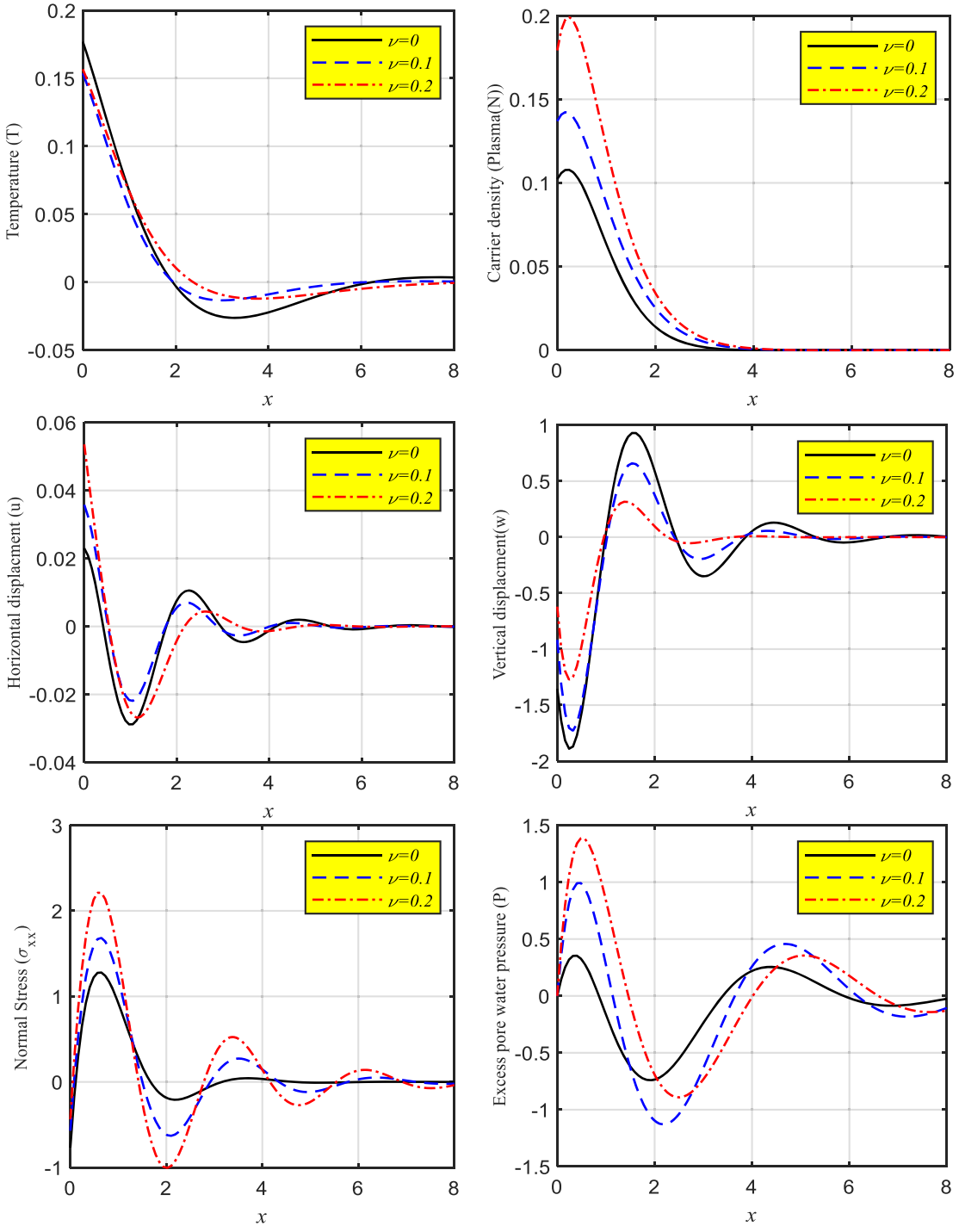

Figure 1: The main physical distributions against the horizontal distance for different distinct values of decaying parameter υ under the effect of LS model at the variable thermal conductivity $K_1 = -0.02$.

further modulated by the variable thermal conductivity (Figure 2), which introduces spatial variations in the carrier distribution. But, the mechanical displacements in both horizontal and vertical directions exhibit strong dependence on the thermal field (decaying heat source). With an increase in the decaying heat parameter, the thermal strain resulting from the temperature field decreases, leading to reduced magnitudes of both horizontal and vertical displacements. This reduction is more pronounced in regions farther from the heat source. The effect of variable thermal conductivity (Figure 2) also plays a critical role, as regions with higher conductivity exhibit

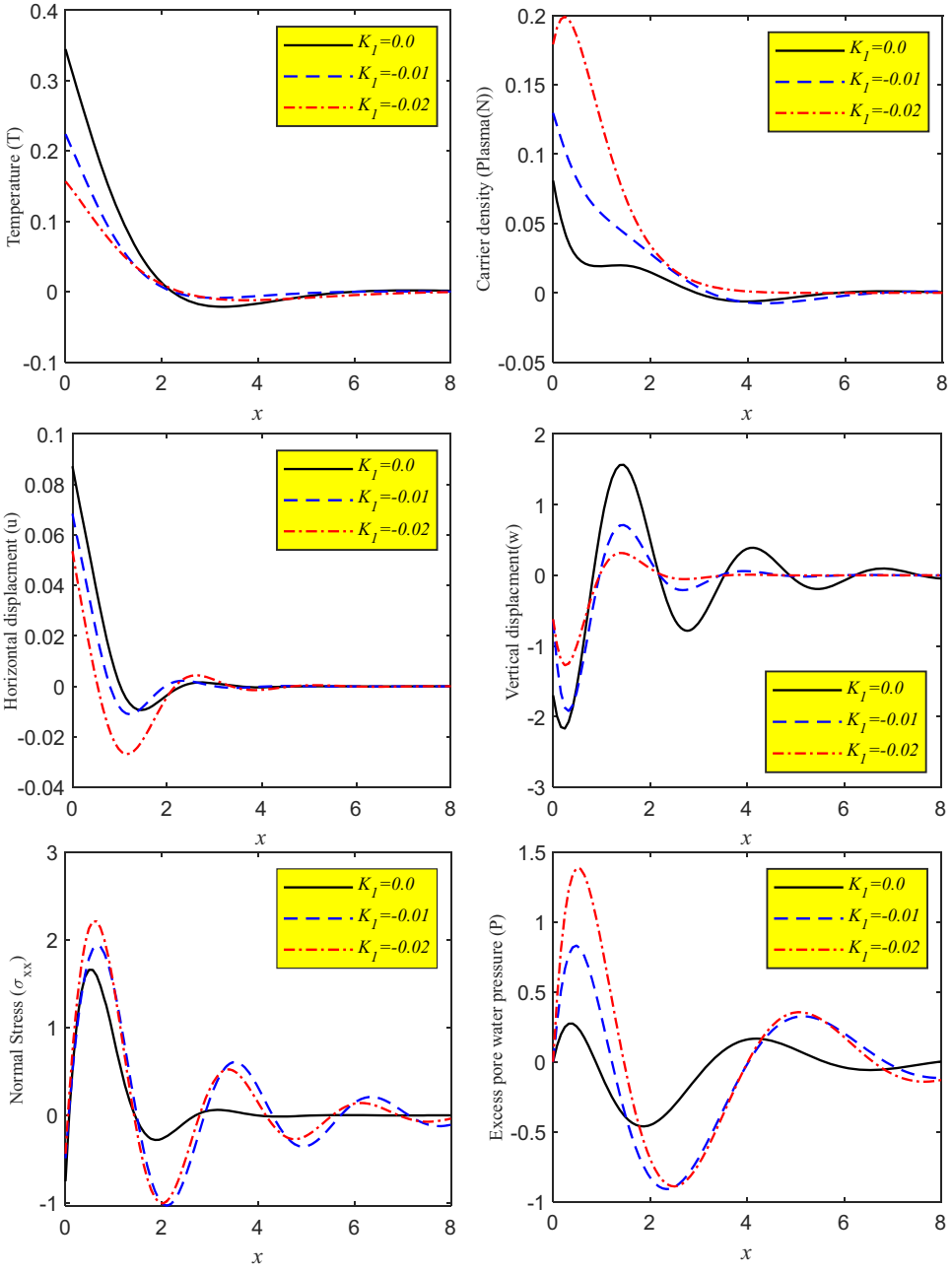

Figure 2: Variation in the main physical distributions against the horizontal distance under the effect of different values of variable thermal conductivity according to the Lord and Shulman (LS) model when the decaying parameter υ = 0.2.

more rapid changes in displacement profiles, indicating stronger localized thermal expansion and contraction. On the other side, the mechanical stress distribution is sensitive to the combined effects of the thermal and elastic fields. As the decaying heat parameter increases, the thermal stress generated within the medium decreases due to reduced thermal gradients. Numerical simulations show that the stress concentration near the heat source is alleviated, leading to a smoother stress distribution throughout the medium. The variable thermal conductivity further alters the stress profile, with areas of higher conductivity showing more pronounced stress relaxation. Finally, in the poroelastic semiconductor medium, excess pore water pressure is influenced by the thermal expansion of the solid matrix and the movement of fluid within the pores. The decaying heat parameter significantly impacts the rate of fluid diffusion. Higher decaying heat parameters result in lower thermal-induced expansion, thereby reducing the

excess pore water pressure generated. The effect of variable thermal conductivity amplifies this behavior, with regions of higher conductivity exhibiting faster dissipation of pore water pressure. In general, the decaying heat parameter plays a crucial role in controlling the wave propagation of various physical fields in the poroelastic semiconductor medium. The interplay between thermal decay and variable thermal conductivity leads to non-uniform distributions of temperature, carrier density, mechanical displacements, stress, and pore water pressure, highlighting the complex thermo-mechanical-electrical coupling in such systems. In this study, we have explored the effects of varying the decaying heat parameter on the thermal, mechanical, and electronic properties of the semiconductor material. Our analysis reveals that as the decaying heat parameter increases, the thermal effects become more localized. This localization is quantified by the sharper temperature gradients observed near the heat source, resulting in a confined region of high thermal activity. The temperature distribution narrows, leading to an increased concentration of thermal effects within a smaller spatial region. This localization also has significant implications for other physical quantities. The carrier density, which is strongly influenced by temperature variations, exhibits pronounced spatial variation as thermal excitation is more concentrated. As the heat becomes more localized, the carrier density response becomes more non-uniform, with higher concentrations near the thermal source. Similarly, the induced thermal stress becomes more localized, with greater concentrations near the region of intense temperature variation. These localized stresses can lead to mechanical deformation or potential failure in certain regions of the semiconductor. Furthermore, the localization of thermal effects impacts the propagation of optical and acoustic waves, as the refractive index and acoustic velocity are both temperature-dependent. The confinement of thermal disturbances results in increased attenuation or scattering of waves within the localized region, altering wave behavior in the material. Thus, the enhanced localization of thermal effects, driven by the decaying heat parameter, not only changes the thermal and stress distributions but also modifies the electronic and wave propagation characteristics of the semiconductor material. Variable thermal conductivity significantly affects wave speed, attenuation, and field coupling. It causes non-uniform wave speeds as higher conductivity regions allow for faster propagation of thermal and mechanical disturbances, while lower conductivity areas slow wave speeds due to thermal gradients. Attenuation increases in regions with lower conductivity, as localized thermal gradients and stresses enhance wave scattering and energy dissipation. Furthermore, variable conductivity affects the coupling between thermal, mechanical, and electromagnetic fields by inducing differential thermal expansion in areas with lower conductivity, leading to stronger thermal-mechanical coupling. Additionally, changes in conductivity can alter material properties like refractive index, modifying the coupling between thermal and electromagnetic fields, especially in regions with poor heat conduction.

6 Comparisons

Table 2 presents a comparative analysis of our model with the prior analytical studies by Lotfy *et al.* [29] and Youssef and El-Bary [32], highlighting the key differences and advancements introduced in our work. Unlike previous models that assumed constant thermal conductivity and either ignored or simplified the heat source, our approach incorporates a temperature-dependent thermal conductivity and a decaying heat source, providing a more comprehensive representation of thermoelastic and plasma interactions in semiconductor media. The table illustrates how these enhancements significantly influence the temperature, stress, and carrier distributions, addressing the limitations of earlier studies. Additionally, the validation of our model is demonstrated by its alignment with prior analytical results when the new parameters are omitted, reinforcing the accuracy and applicability of the proposed technique.

This comparison highlights the advancements in our model and validates its accuracy by showing that our results align with prior studies when the new parameters are excluded.

7 Conclusion

The study highlights the critical role of the decaying heat parameter and variable thermal conductivity on wave propagation phenomena in a poroelastic semiconductor medium, analyzed within the framework of photo-thermoelasticity theory. The decaying heat parameter significantly influences the attenuation and diffusion of thermal waves, thereby impacting the coupled fields of temperature, carrier density, displacements, mechanical stress, and excess pore water pressure. As the decaying heat parameter increases, thermal effects become more localized, leading to reduced mechanical strain, stress, and fluid movement. Furthermore, the inclusion of variable thermal conductivity adds complexity to the wave propagation process,

Table 2: Compare current results with previous ones

Aspect	Our model	Yasein *et al.* [36]	Youssef *et al.* [32]
Heat conduction equation	Modified to include variable thermal conductivity: $K(T) = K_0(1 + K_1T)$ and decaying heat source terms	Standard heat conduction with constant K and no decay effects	Included variable $K(T)$ but without dynamic heat source or plasma effects
Coupling effects considered	THM-plasma coupling with temperature-dependent properties	Thermo-mechanical coupling only	Thermo-mechanical coupling with variable $K(T)$ but no plasma or decaying source
Mathematical approach	Utilized normal mode analysis combined with map transformations for handling nonlinearity	Applied normal mode analysis with linear assumptions	Analytical methods with focus on steady-state solutions
Boundary conditions	Included time-dependent thermal shock and free surface conditions for pore pressure and carrier density	Applied constant or ramp-type thermal boundary conditions	Focused on steady-state boundary conditions with no time dependence
Thermal decay representation	Exponential decay: $T(0, z, t) = T_0e^{-\upsilon t}$	Not considered but thermal ramp type	Not considered, but constant thermal shock
Physical quantities analyzed	Temperature, stress, displacement, carrier density, excess pore water pressure	Temperature, stress, displacement	Temperature, stress, displacement
Numerical implementation	Conducted with MATLAB for solving coupled differential equations	Focused on analytical solutions without detailed numerical analysis	Employed basic numerical methods for steady-state solutions
Impact of variable conductivity	Demonstrated significant impact on temperature gradients, stress distribution, and carrier density profiles	Did not address variable thermal conductivity effects	Recognized impact on temperature but lacked plasma interaction analysis
Key contribution	Provided a unified model capturing decay effects and variable conductivity for hydro-semiconductor systems	Highlighted thermoelastic effects in semiconductors under constant conductivity assumptions	Showed effects of variable conductivity in elastic media without plasma and decay considerations

introducing spatial variations in thermal dissipation, mechanical deformation, and carrier distribution. This combined influence underscores the intricate coupling between thermal, mechanical, and electrical processes in poroelastic semiconductor systems, making the decaying heat parameter and variable thermal conductivity essential factors in understanding and controlling the behavior of such media in practical applications. The effect of the decaying heat parameter and variable thermal conductivity on wave propagation in poroelastic semiconductor media has significant applications in advanced technologies. In general, most sensitive to thermal conductivity: temperature: strongly dependent on conductivity, stress: directly tied to temperature gradients, and wave propagation: sensitive due to changes in material homogeneity. On the other hand, most sensitive to decaying heat parameter: carrier density: highly sensitive to the localization of heat, stress: localized thermal stress is influenced by the rate of heat decay, and wave propagation: sensitivity increases with more localized heating. In semiconductor devices, they are critical for heat management, influencing temperature, carrier density, and mechanical stress distributions, which impact performance and reliability. In nano-devices, controlling these parameters reduces thermal-induced displacements and stress, enhancing precision. In geothermal and subsurface engineering, they affect excess pore water pressure and stress propagation, aiding in resource extraction and infrastructure stability. Additionally, they optimize thermoelectric energy conversion and improve laser-based material processing by controlling thermal and mechanical responses.

Acknowledgments: The author would like to thank Prof. Khaled Lotfy (Zagazig University, Egypt) for his continuous support and constructive contribution to the completion of this work.

Funding information: The author states no funding involved.

Author contribution: The author has accepted responsibility for the entire content of this manuscript and approved its submission.

Conflict of interest: The author states no conflict of interest.

Data availability statement: The datasets generated and/or analyzed during the current study are available from the corresponding author on reasonable request.

References

[1] Mahdy A, Lotfy Kh, El-Bary A, Roshdy E, Abd El-Raouf M. Variable thermal conductivity during the photo-thermoelasticity theory of semiconductor medium induced by laser pulses with hyperbolic two-temperature theory. Waves Random Complex Media. 2021;34(4):2877–99. doi: 10.1080/17455030.2021.1969062.

[2] He C-F, Lu GG, Shan XN, Sun YF, Li T, Qin L, et al. Theoretical analysis of 980 nm high power vertical external-cavity surface-emitting semiconductor laser (VECSEL). In ICO20: Lasers and laser technologies, Int Soc Opt Photon. Vol. 6028, 2005. p. 60280X. doi: 10.1117/12.667161.

[3] Kutbi M, Zenkour A. Modified couple stress model for thermoelastic microbeams due to temperature pulse heating. J Comput Appl Mech. 2022;53(1):83–101. doi: 10.22059/jcamech.2022.334218.669.

[4] Zenkour A, Abouelregal A. Two-temperature theory for a heated semi-infinite solid by a pulsed laser radiation. Arch Thermodyn. 2020;41(2):85–101. doi: 10.24425/ather.2020.133623.

[5] Biot MA. Thermoclasticity and irreversible thermodynamics. J Appl Phys. 1956;27:240–53.

[6] Lord HW, Shulman Y. A generalized dynamical theory of thermolasticity. J Mech Phys Solids. 1967;15:299–306.

[7] Green AE, Lindsay KA. Thermoelasticity. J Elast. 1972;2:17.

[8] Green A, Naghdi P. A reexamination of the basic results of themomechanics. Proc R Soc Lond A. 1991;432:171–94.

[9] Green A, Naghdi P. On undamped heat waves in an elastic solid. J Therm Stresses. 1992;15:252–64.

[10] Tzou DY. A unified field approach for heat conduction from macro to micro scales. ASME J Heat Transf. 1995;117:8–16.

[11] Youssef HM. Theory of two-temperature-generalized thermoelasticity. IMA J Appl Math. 2006;71:383–90.

[12] Hetnarski RB, Ignaczak J. Generalized thermoelasticity. J Therm Stresses. 1999;22:451–76.

[13] Othman M, Abo-Dahab S, Lotfy Kh. Gravitational effect and initial stress on generalized magneto-thermo-microstretch elastic solid for different theories. Appl Math Comput. 2014;230:597–615.

[14] Lotfy Kh. Mode-I crack in a two-dimensional fibre-reinforced generalized thermoelastic problem. Chin Phys B. 2012;21(1):014209.

[15] Ailawalia P, Singh N. Effect of rotation in a generalized thermoelastic medium with hydrostatic initial stress subjected to ramp type heating and loading. Int J Thermophys. 2009;30:2078–97.

[16] Abbas I, Kumar R. Response of thermal source in initially stressed generalized thermoelastic half-space with voids. J Comput Theor Nanosci. 2014;11(6):1472–9.

[17] Bachher M, Sarkr N, Lahiri A. Generalized thermoelastic infinite medium with voids subjected to an instantaneous heat source with fractional derivative heat transfer. Int J Mech Sci. 2014;89:84–91.

[18] Abbas I, Marin M. Analytical solutions of a two-dimensional generalized thermoelastic diffusions problem due to laser pulse. Iran J Sci Technol Trans Mech Eng. 2018;42:57–71.

[19] Marin M, Öchsner A, Bhatti M. Some results in Moore-Gibson-Thompson thermoelasticity of dipolar bodies. (ZAMM) Zfur Angew Math Mech. 2020;100(12):Art No. e202000090.

[20] Gordon J, Leite R, Moore R, Porto S, Whinnery J. Long-transient effects in lasers with inserted liquid samples. Bull Am Phys Soc. 1964;119:501–10.

[21] Kreuzer L. Ultralow gas concentration infrared absorption spectroscopy. J Appl Phys. 1971;42(7):2934–43.

[22] Mandelis A, Nestoros M, Christofides C. Thermoelectronic-wave coupling in laser photothermal theory of semiconductors at elevated temperatures. Opt Eng. 1997;36(2):459–68.

[23] Todorović D. Plasmaelastic and thermoelastic waves in semiconductors. J de Phys IV (Proc). 2005;125:551–5. doi: 10.1051/jp4:2005125127.

[24] Song Y, Todorovic D, Cretin B, Vairac P. Study on the generalized thermoelastic vibration of the optically excited semiconducting microcantilevers. Int J Solids Struct. 2010;47:1871.

[25] Hosseini S, Zhang C. Plasma-affected photo-thermoelastic wave propagation in a semiconductor Love–Bishop nanorod using strain-gradient Moore–Gibson–Thompson theories. Thin-Walled Struct. 2022;179:109480.

[26] Ailawalia P, Sachdeva S, Singh D, Wu Y. Effect of mechanical force along the interface of semi-infinite semiconducting medium and thermoelastic micropolar cubic crystal. Cogent Math. 2017;4(1):1347991. doi: 10.1080/23311835.2017.1347991.

[27] Hobiny A, Abbas I. A GN model on photothermal interactions in a two-dimensions semiconductor half space. Results Phys. 2019;15:102588.

[28] Liu J, Han M, Wang R, Xu S, Wang X. Photothermal phenomenon: Extended ideas for thermophysical properties characterization. J Appl Phys. 2022;131:065107. doi: 10.1063/5.0082014.

[29] Lotfy KH, Elidy E, Tantawi R. Photothermal excitation process during hyperbolic two-temperature theory for magneto-thermo-elastic semiconducting medium. Silicon. 2021;13:2275–88.

[30] Raddadi M, El-Sapa Sh, Elamin M, Chtioui H, Chteoui R, El-Bary A, et al. Optoelectronic–thermomagnetic effect of a microelongated non-local rotating semiconductor heated by pulsed laser with varying thermal conductivity. Open Phys. 2024;22(1):20230145. doi: 10.1515/phys-2023-0145.

[31] Elamin M, El-Sapa Sh, Chtioui H, Chteoui R, Anwer N, El-Bary A, et al. Response of photo-elasto-electric semiconductor porosity medium according to changing thermal conductivity with two-temperature. AIP Adv. 2023;13(12):125018. doi: 10.1063/5.0179872.

[32] Youssef H, El-Bary A. Thermal shock problem of a generalized thermoelastic layered composite material with variable thermal conductivity. Math Probl Eng. 2006;87940:1–14. doi: 10.1155/mpe/2006/87940.

[33] Ezzat M, Youssef H. State space approach for conducting magneto-thermoelastic medium with variable electrical and thermal conductivity subjected to ramp-type heating. J Therm Stresses. 2009;32(4):414–27. doi: 10.1080/01495730802637233.

[34] Sherief H, Abd El-Latief A. Effect of variable thermal conductivity on a half-space under the fractional order theory of thermoelasticity. Int J Mech Sci. 2013;74:185–9.

[35] Zenkour A, Abbas I. Nonlinear transient thermal stress analysis of temperature-dependent hollow cylinders using a finite element model. Int J Struct Stab Dyn. 2014;14(7):1450025. doi: 10.1142/S0219455414500254.

[36] Yasein M, Mabrouk N, Lotfy Kh, EL-Bary A. The influence of variable thermal conductivity of semiconductor elastic medium during

photothermal excitation subjected to thermal ramp type. Results Phys. 2019;15:102766.
[37] Abbas I, Hobiny A, Marin M. Photo-thermal interactions in a semiconductor material with cylindrical cavities and variable thermal conductivity. J Taibah Univ Sci. 2020;14(1):1369–76. doi: 10.1080/16583655.2020.1824465.
[38] Lotfy Kh, El-Bary A. Elastic-thermal-diffusion model with a mechanical ramp type and variable thermal conductivity of electrons–holes semiconductor interaction. Waves in random and complex media; 2022. p. 1–20. doi: 10.1080/17455030.2022.2078521.
[39] Liu H, Wang F. A novel semi-analytical meshless method for the thickness optimization of porous material distributed on sound barriers. Appl Math Lett. 2024;147:108844.
[40] Kumar R, Devi S. Thermomechanical intereactions in porous generalized thermoelastic material permeated with heat sources. Multidiscip Model Mater Struct. 2008;4:237–54.
[41] Sherief H, Hussein E. A mathematical model for short-time filtration in poroelastic media with thermal relaxation and two temperatures. Transp Porous Media. 2012;91:199–223.
[42] Abbas I, Youssef H. Two-dimensional fractional order generalized thermoelastic porous material. Lat Am J Solids Struct. 2015;12:1415–31.
[43] Wei W, Zheng R, Liu G, Tao H. Reflection and refraction of P wave at the interface between thermoelastic and porous thermoelastic medium. Transp Porous Media. 2016;113:1–27.
[44] Schanz M. Poroelastodynamics: Linear models, analytical solutions, and numerical methods. Appl Mech Rev. 2009;62(3):030803. doi: 10.1115/1.3090831.
[45] Marin M, Hobiny A, Abbas I. Finite element analysis of nonlinear bioheat model in skin tissue due to external thermal sources. Mathematics. 2021;9(13):Art. No. 1459.
[46] Abousleiman Y, Ekbote S. Solutions for the inclined borehole in a porothermoelastic transversely isotropic medium. Trans ASME E: J Appl Mech. 2005;72:102–14.
[47] Booker J, Savvidou C. Consolidation around a spherical heat source. Int J Solids Struct. 1984;20:1079–90.
[48] Biot M. Variational Lagrangian-thermodynamics of non-isothermal finite strain mechanics of porous solids and thermomolecular diffusion. Int J Solids Struct. 1977;13:579–97.
[49] Xiong C, Ying G, Yu D. Normal mode analysis to a poroelastic half-space problem under generalized thermoelasticity. Lat Am J Solids Struct. 2017;14(5):930–49. doi: 10.1590/1679-78253611.
[50] Gupta S, Dutta R, Das S, Verma A. Double poro-magneto-thermoelastic model with microtemperatures and initial stress under memory-dependent heat transfer. J Therm Stresses. 2023;46(8):743–74. doi: 10.1080/01495739.2023.2202718.
[51] Dutta R, Das S, Gupta S, Singh A, Chaudhary H. Nonlocal fiber-reinforced double porous material structure under fractional-order heat and mass transfer. Int J Numer Methods Heat Fluid Flow. 2023;33(11):3608–41. doi: 10.1108/HFF-05-2023-0295.
[52] Dutta R, Das S, Bhengra N, Kumar S, Karma V, Das S. Nonlocal effect on shear wave propagation in a fiber-reinforced poroelastic layered structure subjected to interfacial impulsive disturbance. Soil Dyn Earthq Eng. 2024;176:108307. doi: 10.1016/j.soildyn.2023.108307.
[53] Meghana R, Dutta R, Gupta V, Singhal A, Craciun E, Das S. Size-dependent analysis of surface wave in irregular fractured porous seabed subjected to fractional-order derivative. Mech Adv Mater Struct. 2025;1–22. doi: 10.1080/15376494.2024.2440131.
[54] Das S, Dutta R, Gupta V, Singhal A, Barak M, Almohsen B. Fractional and effects on wave reflection in pre-stressed microstructured solids with dual porosity. Eur J Mech - A/Solids. 2025;111:105565. doi: 10.1016/j.euromechsol.2024.105565.
[55] Gupta V, Barak M, Ahmad H, Das S, Almohsen B. Response of moisture and temperature diffusivity on an orthotropic hygro-thermo-piezo-elastic Medium. J Nonlinear Math Phys. 2024;31:26. doi: 10.1007/s44198-024-00187-z.
[56] El-Sapa Sh, Lotfy Kh, Elidy E, El-Bary A, Tantawi R. Photothermal excitation process in semiconductor materials under the effect moisture diffusivity. Silicon. 2023;15:4171–82.
[57] Sharma A, Sharma J, Sharma Y. Modeling reflection and transmission of acoustic waves at a semiconductor: Fluid interface. Adv Acoust Vib. 2012;2012:637912.
[58] Mahdy A, Gepreel Kh, Lotfy Kh, El-Bary A. A numerical method for solving the Rubella ailment disease model. Int J Mod Phys C. 2021;32(7):2150097. doi: 10.1142/S0129183121500972.
[59] Lata P, Heena. Thermomechanical interactions in a transversely isotropic thermoelastic media with diffusion due to inclined load. 2024;90(3):263–72.